In-situ observation of bainite-to-austenite transformation during simulated welding cycle of a micro-alloyed high strength steel

X. W. Lei[1], Honghong Wang[1]*, K. M. Wu[1], Amir A. Shirzadi[1], Y. Q. Yin[2], N. C. Wu[2]

[1] Hubei Collaborative Innovation Center for Advanced Steels,

International Research Institute for Steel Technology,

Wuhan University of Science and Technology, Wuhan 430081, China

[2] Nanjing Iron & Steel Group Co., Ltd., Nanjing 210035, China

* Corresponding author. Tel.: +86 159 7205 0884; Fax: +86 27 68862606;

E-mail: wanghonghong@wust.edu.cn

Abstract: A confocal scanning laser microscope, equipped with a high temperature stage, was used for in-situ observation of the bainite-to-austenite transformation in a micro-alloyed ultra-high strength steel. Austenite grain growth was observed and measured directly from 1040 °C to the peak temperature of 1340 °C during the heating process, as well as the subsequent cooling down to 1040 °C. The grain growth rate versus temperature was analyzed. It was demonstrated that the austenite grains grew up simultaneously by means of grain boundary migration and "grain swallowing" phenomena. The variation in grain growth rate was attributed to the presence of impeding precipitates e.g. carbonitrides Nb,Ti(C,N). The work also showed that coarsening and/or dissolution of carbonitride precipitates, above a certain temperature, led to a fast grain growth. The in-situ observation by confocal scanning laser microscope can provide valuable information on the austenite reformation and final microstructure of weldments.

Key-words: grain growth; bainite to austenite transformation; confocal scanning laser microscope; micro-alloyed steel

1. Introduction

Formation of the high temperature austenitic phase is an inevitable occurrence during heat treatment and welding thermal cycle for vast majority of commercial steels. Austenite generally decomposes into pearlite, ferrite, bainite and martensite during cooling from high temperature to room temperature. Its initial grain size is critical to development of final microstructures and mechanical properties. It was reported that a critical austenite grain size favored acicular ferrite nucleation which was benefit for acicular ferrite formation[1-3]. S. J. Lee et al.[4] demonstrated that bainite transformation temperatures (both B_s and B_f) decreased with decreasing austenite grain size in low alloy steels. The effect of austenite grain size on strength can be estimated using the equations proposed by Hall-Petch or C. H. Young and H. K. D. H. Bhadeshia[5]. The study on microstructures and mechanical properties of pipeline steels by J. Zhu et al.[6] and of ultra-high pipeline steels by H. H. Wang et al.[7] showed that the heat-affected zones (HAZ) with coarse grains had lower impact toughness than the base metal.

It had been suggested that the original microstructure, ferritic-pearlitic and martensite, affected reverse transformation by increasing or decreasing transformation temperature of A_{c1} and A_{c3}[8], while the morphology and grain size of initial phase also had a notable influence on the transformation rate[9]. H. Takuya et al.[10] found that the nucleation and growth of the regenerated austenite predominantly occurred on the grain boundaries of the parent austenite. Also, T. A. Palmer and J. W. Elmer[11] indicated austenite nucleated at sub-boundaries of ferrite. In terms of alloys composition, G. Miyamoto et al.[12] discovered that the addition of Mn, Si and Cr elements retarded austenite reformation by decreasing the carbon activity.

Most of previous researches on re-austenite grain growth behavior were based on the isothermal test cycles with different soaking temperatures, isothermal times and/or heating rates. For example, L.N. Duan et al.[13] studied the austenite grain growth behavior for Nb-Ti microalloyed X80 pipeline steel through changing soaking temperature and soaking time, and revealed that the prior austenite grains grew obviously with the increase of soaking temperature higher than 1180 °C and soaking time longer than 1 h to 3 h. Y.W. Xu et al.[14] also investigated the isothermal austenite grain growth kinetics of hot rolled dual phase steel and developed the empirical model for isothermal austenite grain. However, these researches are incapable of providing information for austenite grain growth on continuous heating process which is more important to understand the reverse transformation. What was more exciting was that laser scanning confocal microscopy (LSCM) was introduced to *in-situ* observe austenite reformation during a simulated welding cycle by S. Takahiro et al.[15] and found out the addition of boron restricted the growth of austenite grains at high temperatures. D. Zhang et al.[16] also used LSCM for the observation of nucleation of intragranular acicular ferrite in simulated welding cycles, and removed the difficulty in observing directly the acicular ferrite formation behavior in micro-alloyed steels. These studies showed the advantage of LSCM in reverse transformation investigation clearly.

In the present work, a high-temperature confocal laser microscope was used to study the effect of micro-alloying elements on the growth rate of austenite grains during a heating cycle similar to that of a conventional welding process. The test data was analyzed and used to provide an in-depth understanding of the phase transformation during welding processes.

2. Experimental

The investigated material in this work is a micro-alloyed high strength steel and its chemical composition is shown in Table 1. This steel exhibits high strength by typical thermo-mechanical controlled process and then tempered at approximately 550°C for about 1 h.

Table 1 Chemical composition (wt.%) of the steel studied in this work

C	Mn	P	S	Si	Mo	Ni+Cr+Cu	Nb+V+Ti+Zr
0.04-0.06	1.5-2.0	≤0.004	≤0.001	0.08-0.10	0.2-0.4	0.8-1.2	0.09-0.12

A confocal He-Ne laser scanning microscope (CLSM, VL2000DX-SVF17SP) with infrared image furnace was used for *in-situ* observation of bainite-to-austenite transformation at elevated temperature during a simulated welding cycle. Schematic illustration of CLSM was described in detail in the literature 15. The microscope used the purple laser scanning illumination imaging technology, the wavelength was 408 nm, and scanning speed was 120 frames per second, the highest resolution was 0.14 μm. The CLSM samples, with approximate 4 mm in diameter and 6 mm in height, were carefully machine-polished, and then set into an alumina crucible. The temperature was controlled through a thermo-couple on the bottom of the aluminum crucible. The sample chamber was pumped vacuum and then filled with argon to prevent the sample from being oxidized during heating. Using focused infrared light heating mode, the specimens were heated to the peak temperature of 1340 °C at the rate of 7 °C s^{-1}, and then cooled down to 500 °C at the rate of 8 °C s^{-1}. The live pictures were taken every fifteenth second from 240 μm × 240 μm surface areas.

The microstructure at room temperature was examined by optical microscopy (OM BM51) and transmission electron microscopy (TEM, JEM 2010 HT). Energy dispersive X-ray spectroscopy (EDX) was used to identify the carbonitrides. The OM specimen was polished using standard techniques and etched in 4 vol.-% nital solution. The preparation of TEM specimen started with slicing a 3 mm diameter rod into 100 μm thick discs. Each disc was ground down to 50 μm using 2000 grit silicon carbide paper, followed by electro-polishing at 50 V at room temperature using a twin-jet unit. The electrolyte consisted of 5 % perchloric acid, 15 % glycerol and 80 % methanol. The austenite grain size was measured by applying the linear intercept method on the pictures taken at the temperature above 1040 °C, during both heating and cooling stages.

3. Results and discussion

3.1 Initial bainitic microstructure

Fig. 1 shows the microstructure of investigated steel in the as-received condition, which predominantly consists of pancake shape bainite laths with a thickness of about 1 μm. Some precipitates with about 40 nm dimensions in either square or round-shapes are observed in the TEM micrograph shown in Fig. 2. EDX results reveal that these precipitates are mostly Nb and Ti carbonitrides. The presence of these finely dispersed carbonitrides is accounted for the high strength and impact toughness of this group of steels. These carbonitrides was suggested to retard the austenite grain growth in the HAZ during welding cycles[17].

The precipitates are likely to be coarsened and dissolved during continuous heating process. The equilibrium thermodynamic calculations using JMatPro software, shown in

Fig. 3, indicates that Nb,Ti(C,N) particles start to dissolve when the temperature goes up above 1070 °C.

3.2 Reformation of austenite at high temperatures

The CLSM micrographs in Fig. 4 were taken at elevated temperatures and they clearly show that some austenite grain boundaries are moving and some are disappearing during the continuous heating process. Grain 1 grows up by grain boundaries migration clearly on heating from 1220 ºC to 1338 ºC (shown in Figs. 4a, 4b and 4c). At the same time, the grain boundaries of grain 2 become vanished gradually, which indicates the typical "grain swallowing" mode. Similarly, grain 3 grows up by swallowing the ambient grains during both heating and initial cooling, as clearly shown in Figs. 4b, 4c and 4d. The previous work showed that austenite grains grew up by boundary migration[18] and "grain swallowing"[19] which was consistent with the observations in this work.

3.3 Mechanisms controlling austenite growth

The grain size was measured in 20 °C steps with the live pictures using the linear intercept method. The average austenite grain size and growth rate are shown in Fig. 5. It shows that the austenite grains grow at 3 different rates as the temperature is steadily increased from 1040 °C to the maximum of 1340 °C (slow Stages 1 & 3 and fast Stage 2). Therefore, two mechanisms are involved in controlling the grain growth rate during the heating stage, as discussed in details below. The first "hindering" mechanism keeps the grain growth rate steady and relatively low during the heating stage below 1180 °C (Stage 1). Following a fast grain growth in Stage 2, the second "hindering" mechanism becomes active above 1240 °C and the growth rate plummets in Stage 3. The reduction in

the growth rate during the subsequent cooling (beyond Stage 3) is expected and is not of interest. A slight delay between the start of cooling stage and reduction in the grain growth rate could be due to experimental error, particularly in the data acquisition speed and feedback loop. The austenite reformation during heating and cooling cycle is schematically illustrated in Fig. 6.

First grain growth "hindering" mechanism: Small precipitates in steel matrix, such as carbonitrides, can restrict austenite grain boundary movement *i.e.* by pinning the grain boundaries. The pinning force is governed by the volume fraction of the particles (*f*) and their size (mean particle radius *r*) as given by C. S. Smith[20] in the following equation.

$$P_Z = \beta \frac{\gamma \cdot f}{r} \quad (1)$$

where β is a dimensionless constant, γ is the grain boundary energy. The equilibrium phase transformation diagram shows that Nb,Ti carbonitrides become unstable above 1070 °C. When the temperature is as high as 1180 °C, Nb,Ti carbonitrides begins to dissolve, hence their pinning effect starts to decline. This may explain the sudden increase in the slope of the grain size curve from Stage 1 to Stage 2.

Second grain growth "hindering" mechanism: The grain growth slows down again when the average grain size exceeds 20 μm in Stage 3. With little or no pinning effect from the carbonitrides, the sluggish grain growth in Stage 3 can be due to the reduction in the free energy available to grow further the already large grains. P. Hellman and M. B. Hillert[21] and B. R. Patterson and Y. Liu[22] estimated the driving force for grain growth as a function of the mean volumetric grain diameter (*D*), grain boundary energy (γ):

$$P_d = \alpha \frac{\gamma}{D} \quad (2)$$

where α is a dimensionless geometric constant. This equation shows that the driving force

reduces as the grains reach certain size and this is due to having grains with a relatively high volume to surface energy ratio.

Since it is the pinning force of Nb, Ti carbonitrides and reduction of driving force that controlling the growth rate of austenite grains at the different growth stages, the similar trend of growth rate will be shown at any heating rate. So the result can be applied for simulation of welding.

4 Conclusions

A CSLM was used to take live pictures of the reformation of austenite in a micro-alloyed steel throughout a simulated welding thermal cycling. Based on the *in-situ* observations the following conclusions are made:

(1) New austenite grains grew simultaneously by grain boundary migration and "grain swallowing" mechanism as the temperature increased.

(2) The growth rates varied throughout the thermal cycle with a slow rate at the beginning followed by a rapid growth and finally entered second slow growth stage to the peak temperature.

(3) The relatively slow growth rate of austenite grains in the first stage was due to the pinning effect of Nb,Ti(C,N) carbonitrides. The coarsening and dissolution of these carbonitrides allowed a rapid grain growth. And the second reduction in the grain growth rate occurred due to reduction in the free energy to grow already large grains.

Acknowledgements

Authors are grateful for the financial support from the *International Science and Technology Cooperation Program of China* under grant No. S2012ZR0211 and *Hubei*

Provincial Department of Science and Technology under grant No. 2012BAA14005.

References：

1. F. J. Barbaro, P. Kraukalis, K. E. Easterling: 'Formation of acicular ferrite at oxide particles in steels', *Mater. Sci. Technol.*, 1989, **5**, (11), 1057-1068.
2. J. L. Lee, Y. T. Pan: 'Microstructure and toughness of simulated heat-affected zone in Ti- and Al-killed steels', *Mater. Sci. Eng., A*, 1991, **136**, 109-119.
3. G. Thewlis: 'Transformation kinetics of ferrous weld metals', *Mater. Sci. Technol.*, 1994, **10**, (2), 110-125.
4. S. J. Lee, J. S. Park, Y. K. Lee: 'Effect of austenite grain size on the transformation kinetics of upper and lower bainite in a low-alloy steel', *Scripta Mater.*, 2008, **59**, 87-90.
5. C. H. Young, H. K. D. H. Bhadeshia: 'Strength of mixtures of bainite and martensite', *Mater. Sci. Technol.*, 1994, **10**, 209-214.
6. J. Zhu, L. Xu, W. Chang, L. H. Hu, M. X. Lu: 'Microstructures and mechanical properties of welded joints of novel 3Cr pipeline steel using an inhouse and two commercial welding wires', *Mater. Des.*, 2014, **53**, 405-411.
7. H. H. Wang, K. M. Wu, X. W. Lei, Y. Qian: 'Effect of fast cooling process on microstructure and toughness of heat-affected zone in high strength pipeline steel X120', *Sci. Technol. Weld. Join.*, 2012, **17**, (4), 309-313.
8. N. A. Nikishov, A. M. Sokolov, V. G. Ul′yanov: 'Influence of heating rate on the alpha→gamma-transformation critical temperatures in 40 Kh steel', *Met. Sci. Heat Treat.*, 1992, **33**, (7-8), 561-564.
9. J. H. Park, Y. K. Lee: 'Non-isothermal austenite formation behavior in an

interstitial free steel with different ferrite microstructures', *Scripta Mater.*, 2008, **58**, 602-605.

10. H. Takuya, M. Naoki, S. Yasuhiro, A. Hitoshi, S. Genichi, S. Masaaki, K. Toshihiko: 'Abnormal α to γ transformation behavior of steels with a martensite and bainite microstructure at a slow reheating rate', *ISIJ Int*., 2009, **49**, (11), 1792-1800.
11. T. A. Palmer, J. W. Elmer: 'Direct observations of the formation and growth of austenite from pearlite and allotriomorphic ferrite in a C-Mn steel arc weld', *Scripta Mater.*, 2005, **53**, 535-54.
12. G. Miyamoto, H. Usuki, Z. D. Li, T. Furuhara: 'Effects of Mn, Si and Cr addition on reverse transformation at 1073 K from spheroidized cementite structure in Fe-0.6mass%C alloy', *Acta Mater.*, 2010, **58**, 4492-4505.
13. L. N. Duan, J. M. Wang, Q. Y. Liu, X. J. Sun, J. C. Cao: 'Austenite grain growth behavior of X80 pipeline steel in heating process', *Journal of Iron and Steel Research, International*, 2010, **17**, (3), 62-66.
14. Y. W. Xu, D. Tang, Y. Song, Z. G. Pan: 'Prediction model for the austenite grain growth in a hot rolled dual phase steel', *Mater. Des*., 2012, **36**, 275-278.
15. S. Takahiro, S. Masatsugu, T. Susumu, T. Kaneaki, A. Yoshitaka, H. Toshihiro, A. Fujio: 'Reverse transformation behavior in B containing high Cr heat resistant steel HAZ', Proc. 8th Int. Conf. on 'Trends in Welding research', Georgia, USA, June 2008, ASM International, Paper 53, 284-291.
16. D. Zhang, H. Terasaki, Y. Komizo: 'In situ observation of the formation of intragranular acicular ferrite at non-metallic inclusions in C－Mn steel', *Acta*

Mater., 2010, **58**, 1369-1378.

17. J. Moon, C. Lee: 'Behavior of (Ti, Nb)(C, N) complex particle during thermomechanical cycling in the weld CGHAZ of a microalloyed steel', *Acta Mater.*, 2009, **57**, (7), 2311-2320.
18. C. García de Andrés, F. G. Caballero, C. Capdevila, D. San Martín: 'Revealing austenite grain boundaries by thermal etching: advantages and disadvantages', *Mater. Charact*., 2003, **49**, 121-127.
19. M. Q. Yan, H. Qian, P. Yang, W. M. Mao, Q. W. Jian, W. X. Jin: 'Analysis of micro-texture during secondary recrystallization in a Hi-B electrical steel', *J. Mater. Sci. Technol*., 2011, **27**, (11), 1065-1071.
20. G. S. Rohrer: 'Introduction to Grains, Phases, and Interfaces-an Interpretation of Microstructure', Trans. AIME, 1948, vol. 175, pp. 15-51, by C.S. Smith', *Metall. Mater. Trans. A*, 2010, **41A**, 2010-1063.
21. P. Hellman, M. Hillert: 'Effect of second-phase particles on grain growth', *Scand. J. Metall*., 1975, **4**, 211-219.
22. B. R. Patterson, Y. Liu: 'Relationship between grain boundary curvature and grain size', *Metall. Trans. A*, 1992, **23**, (9), 2481-2482.

Figure Captions

Fig. 1 (a) Optical and (b) TEM micrographs of investigated steel in the as-received condition.

Fig. 2 TEM and EDX results show the size, distribution and chemical composition of Nb,Ti(C,N) precipitates.

Fig. 3 Dissolution of Nb,Ti(C,N) precipitates at high temperatures - calculated using JMatPro Software.

Fig. 4 Growth and annihilation of austenite grains during a thermal cycle, (a) 1220 °C, (b) 1300 °C and (c) 1338 °C on heating, (d) 1300 °C on cooling.

Fig. 5 Austenite grain size and growth rates during the thermal cycle.

Fig. 6 Schematic illustration of austenite reformation under a typical welding thermal cycle.

Non-colour figure
Click here to download high resolution image

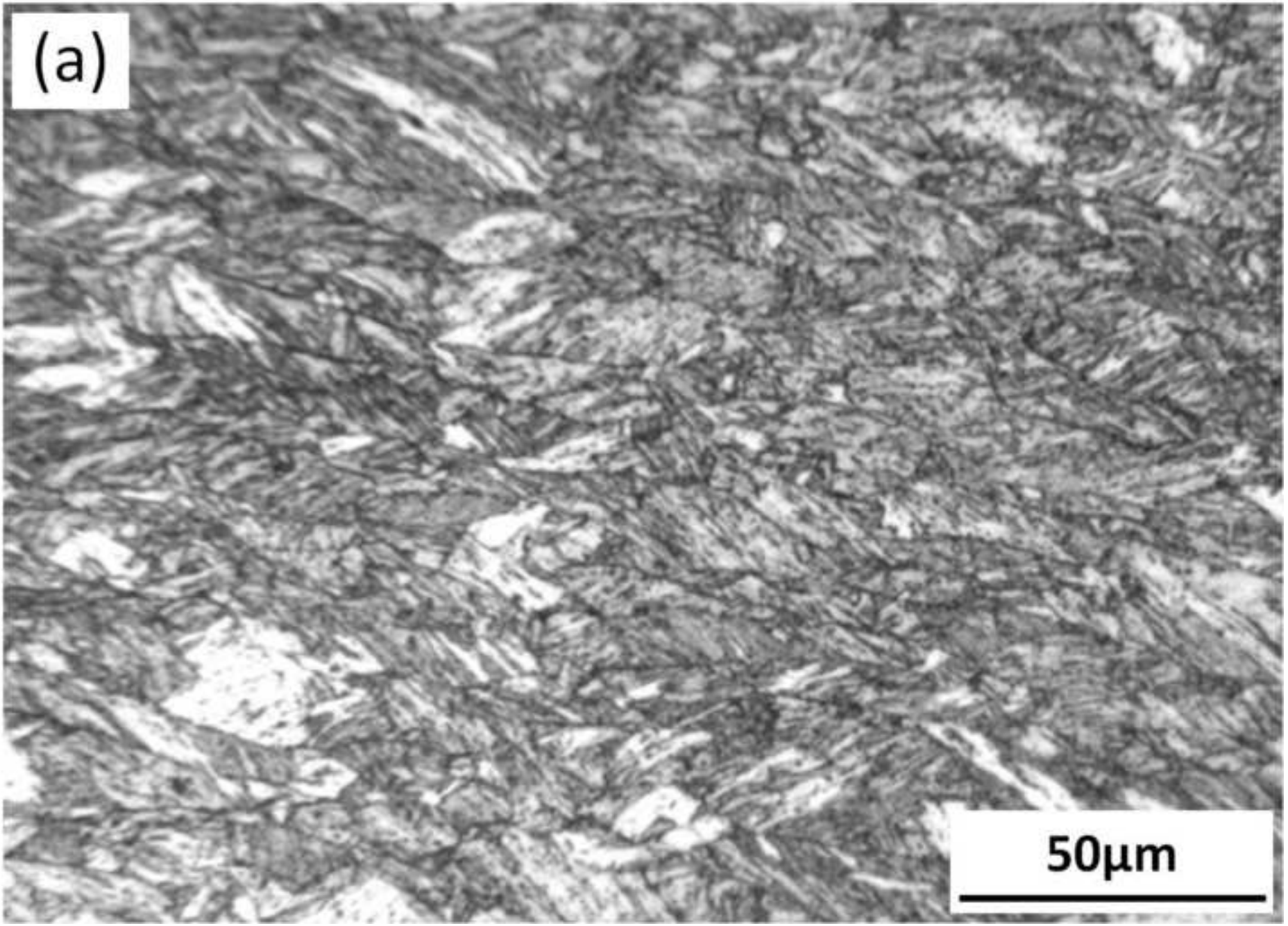

Non-colour figure
Click here to download high resolution image

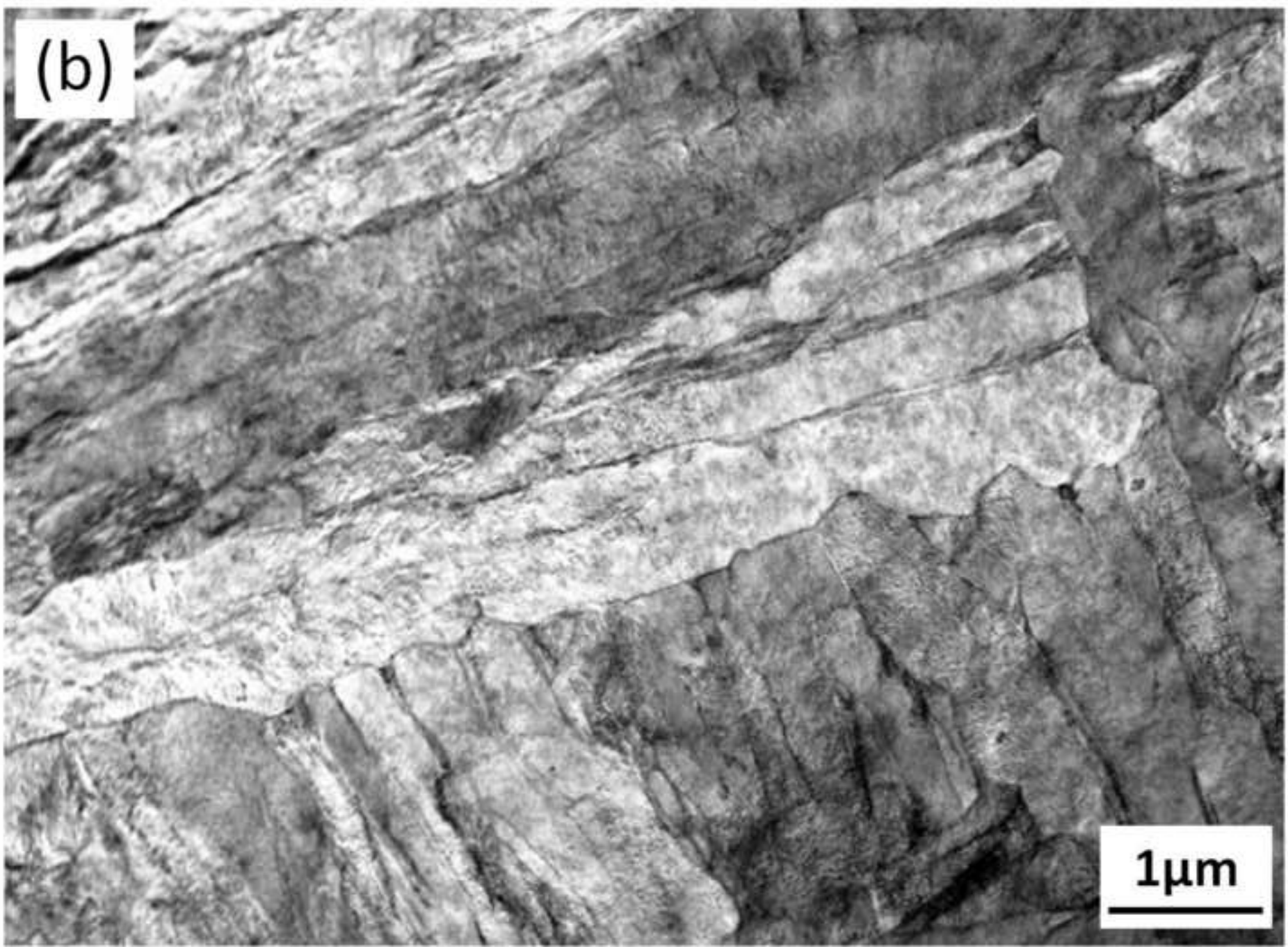

Non-colour figure
Click here to download high resolution image

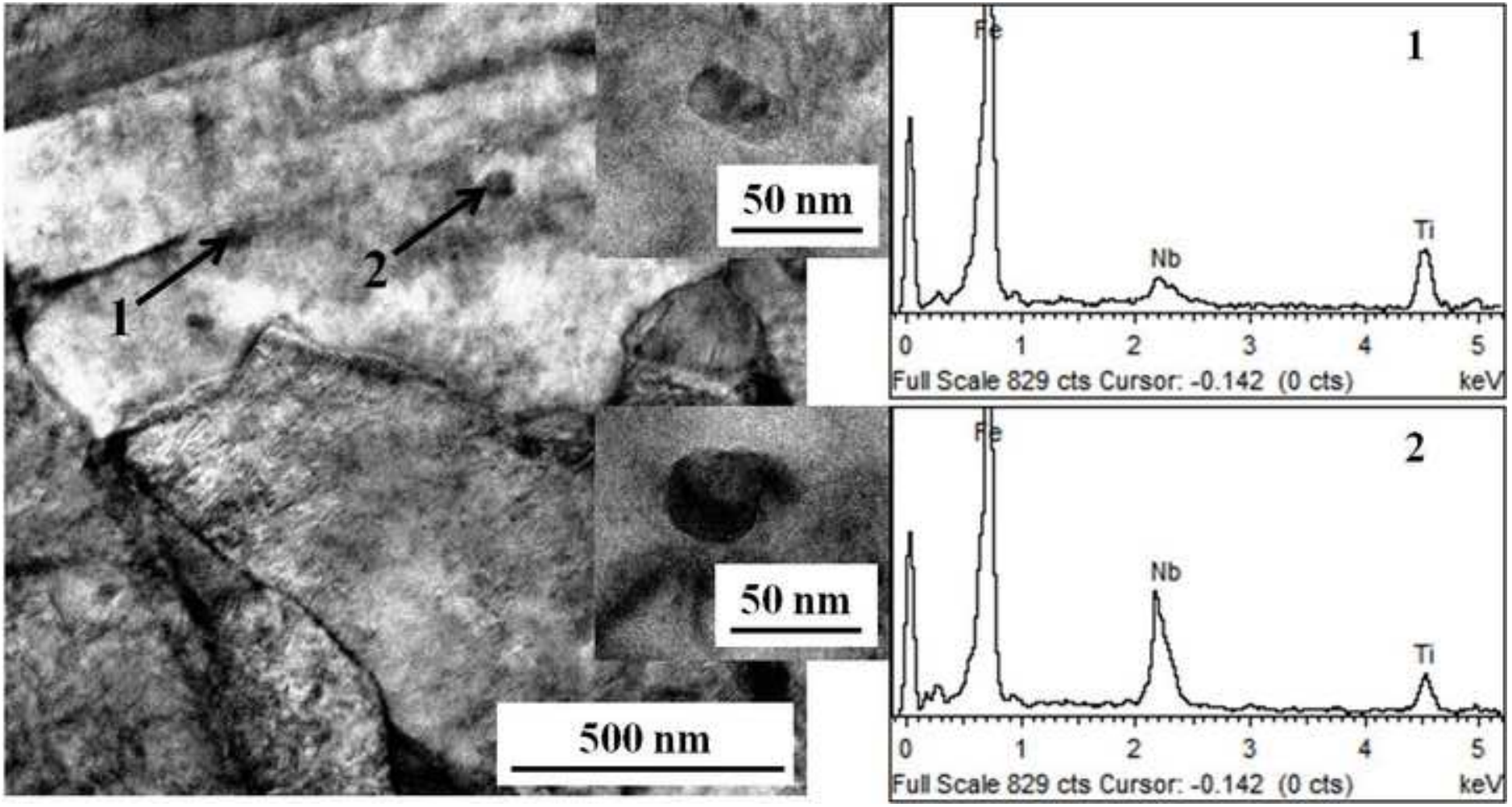

Non-colour figure
Click here to download high resolution image

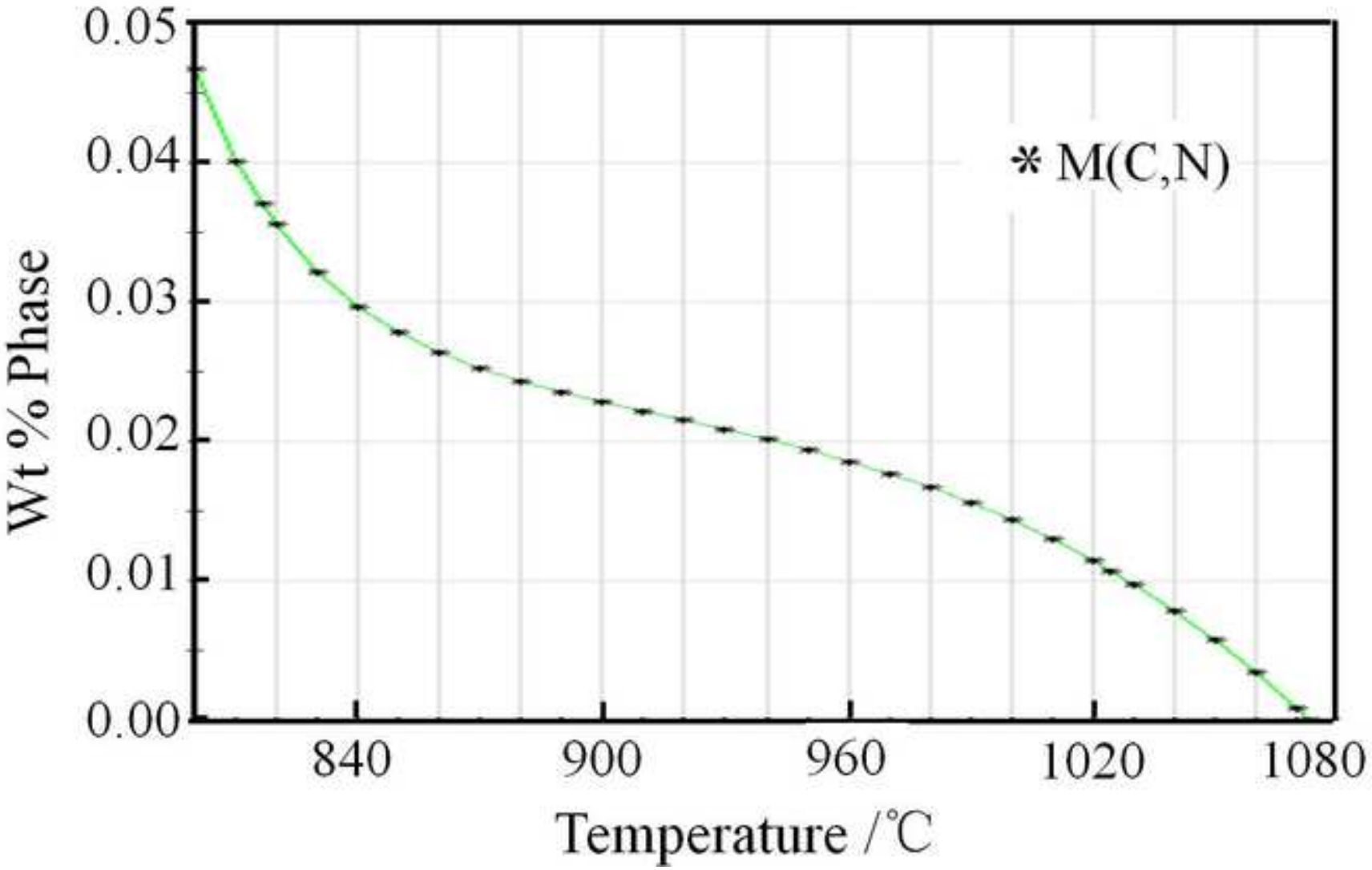

Non-colour figure
Click here to download high resolution image

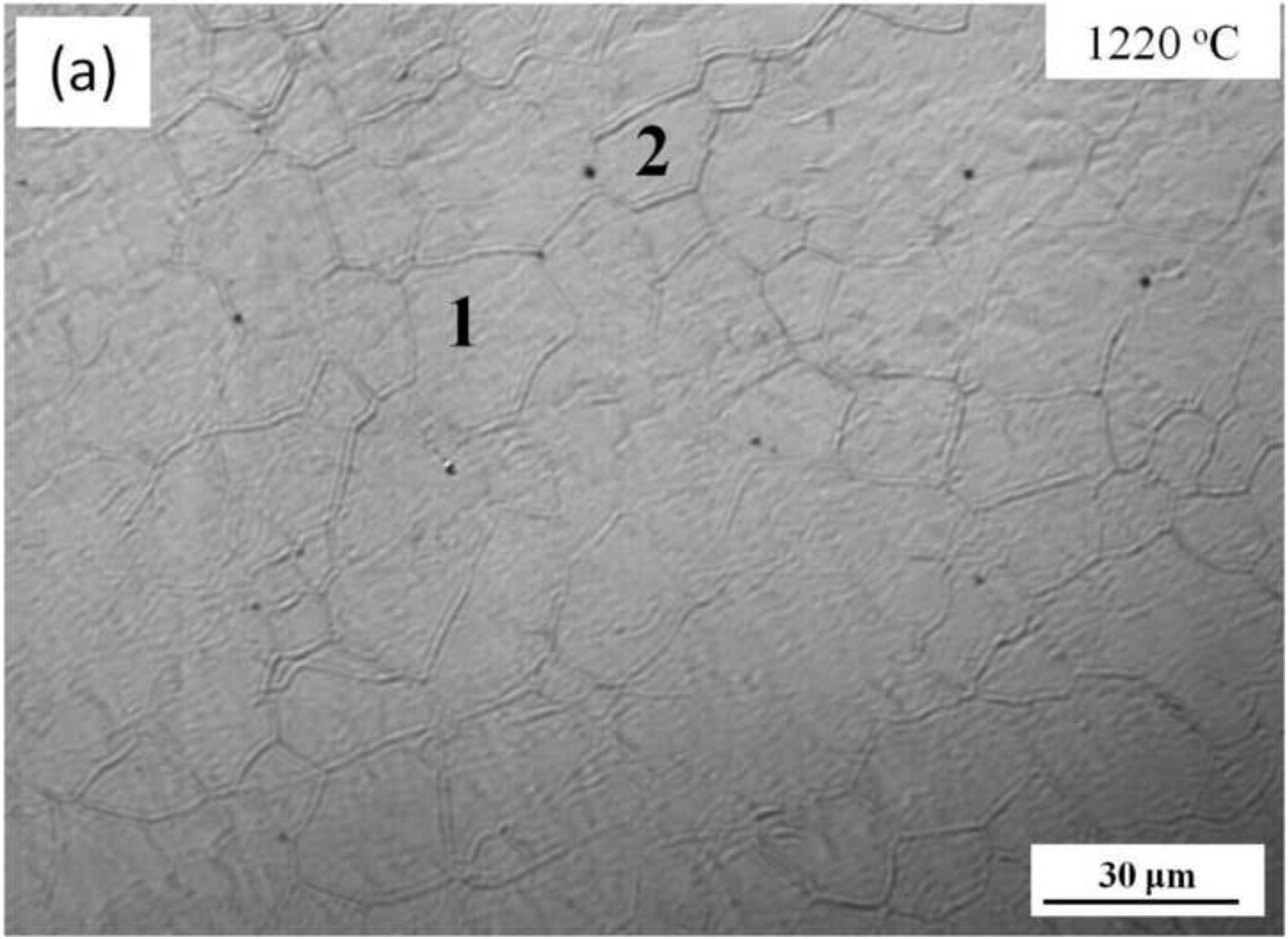

Non-colour figure
Click here to download high resolution image

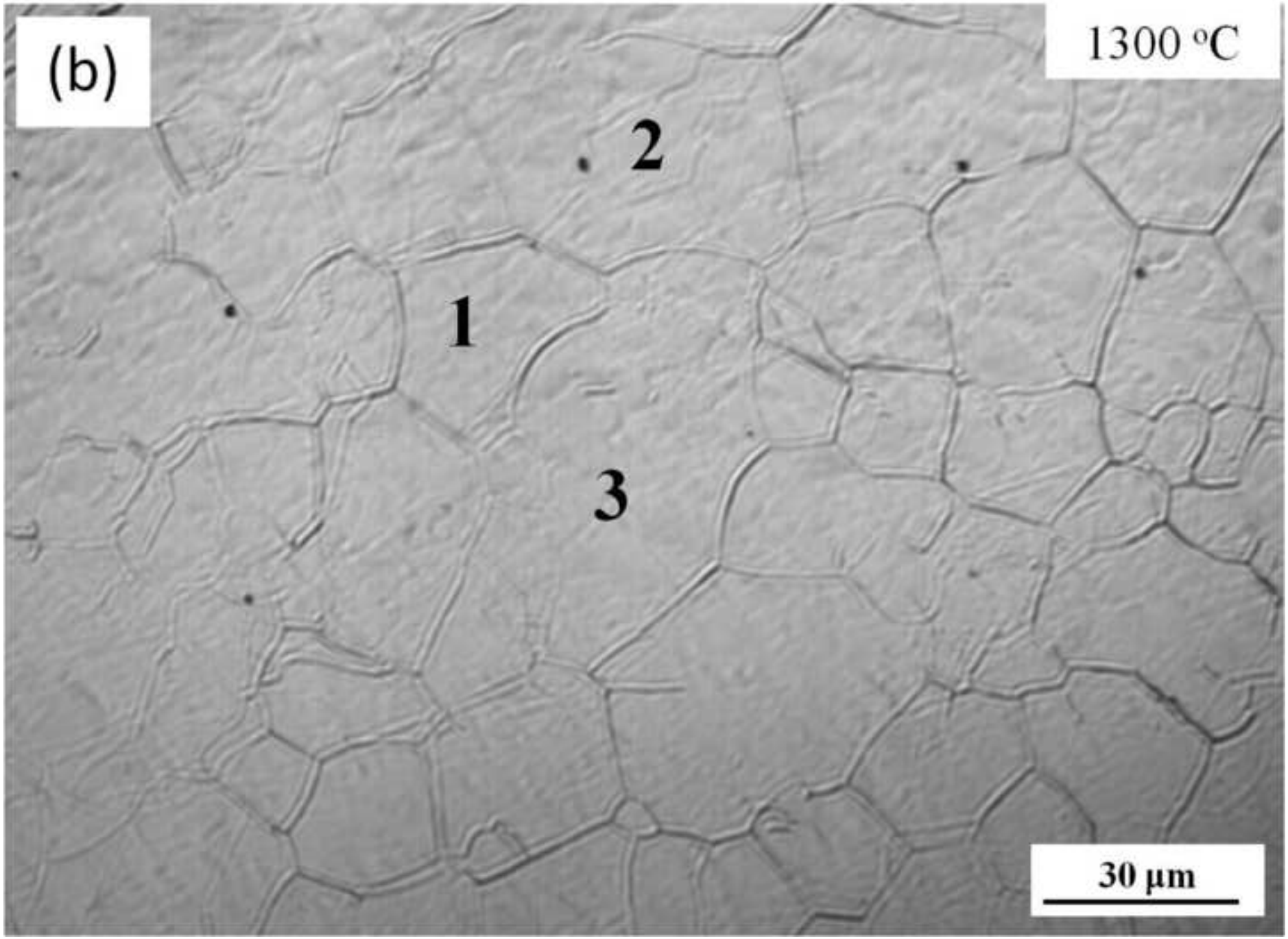

Non-colour figure
Click here to download high resolution image

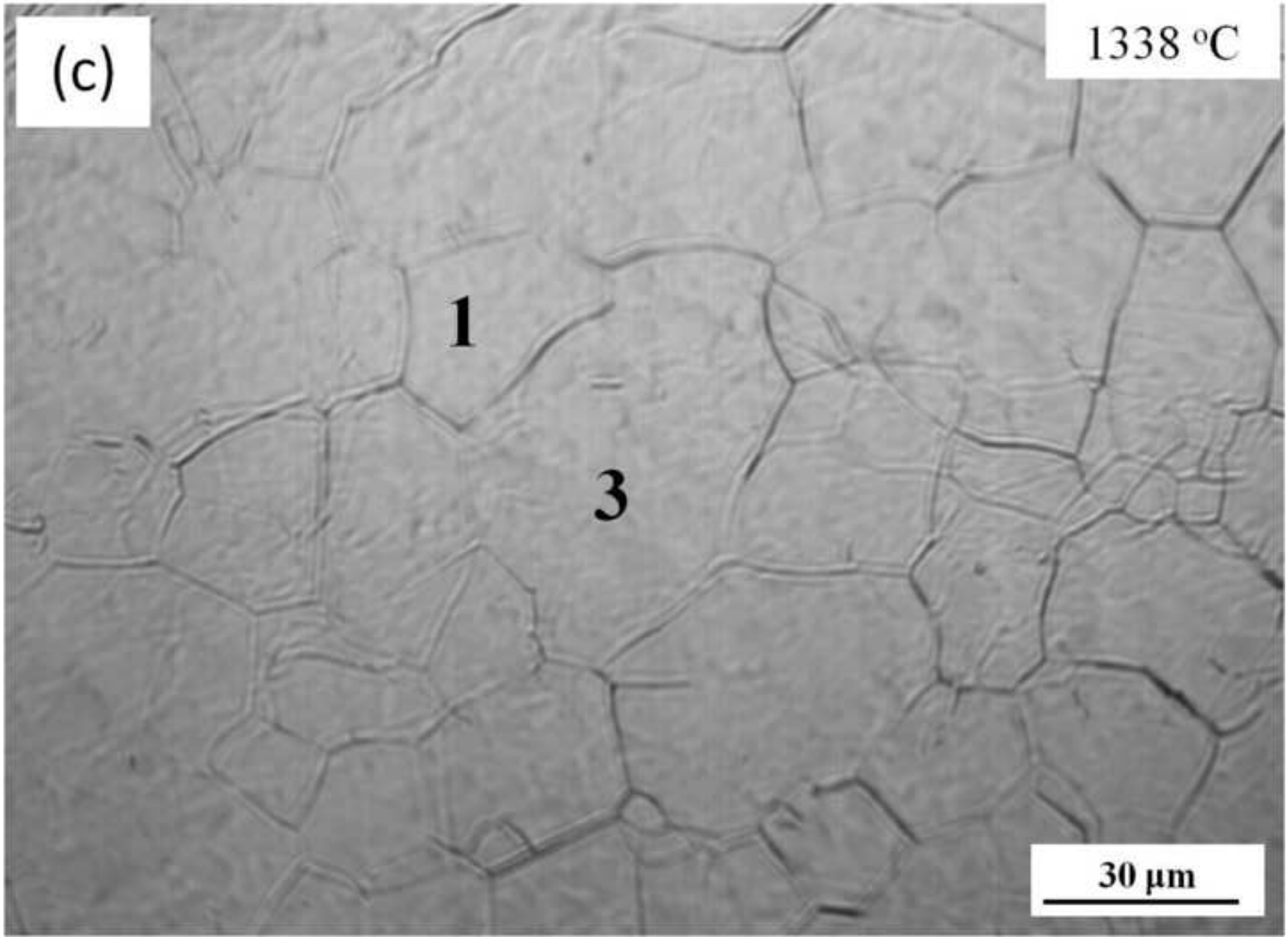

Non-colour figure
Click here to download high resolution image

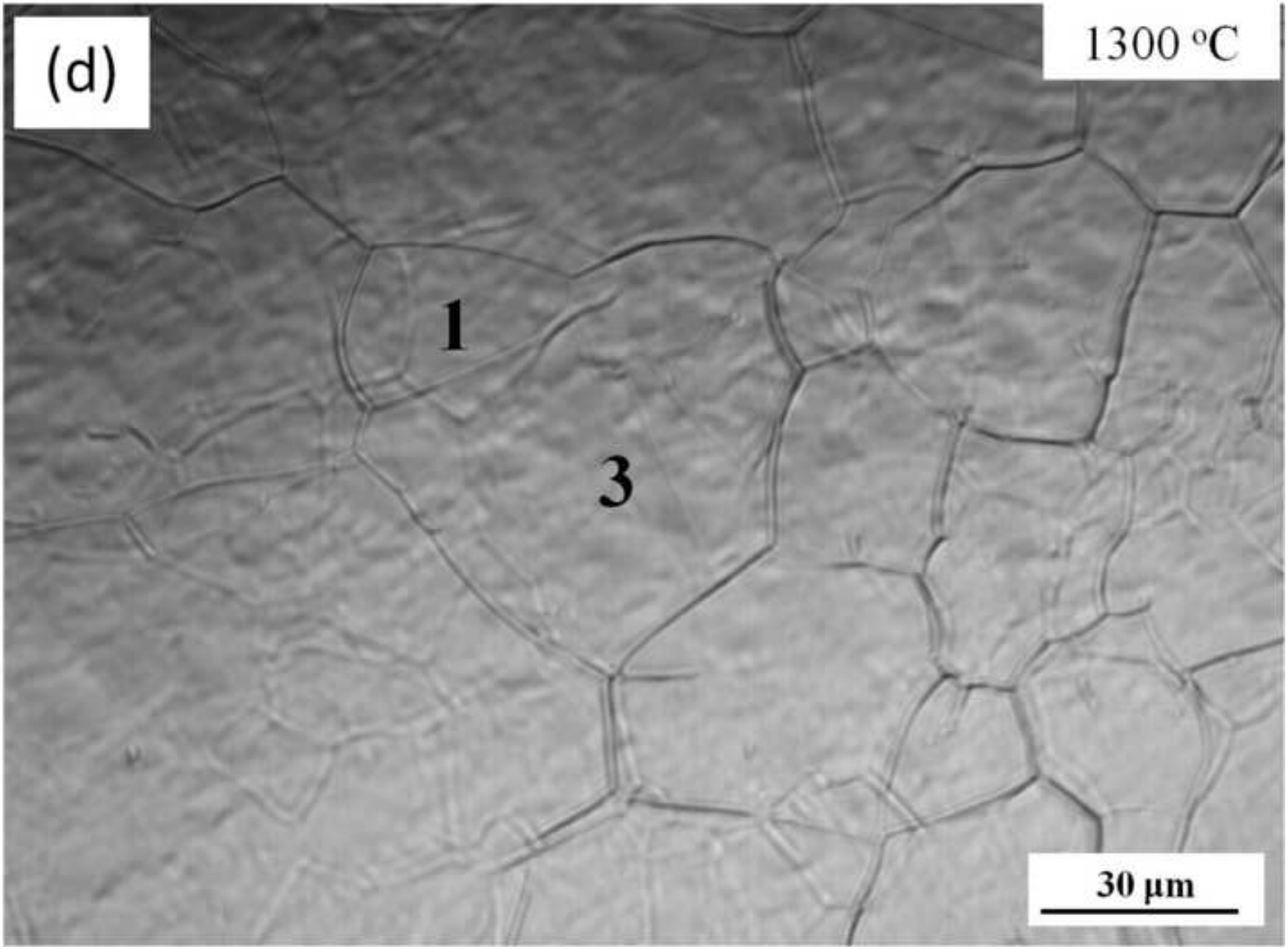

Non-colour figure
Click here to download high resolution image

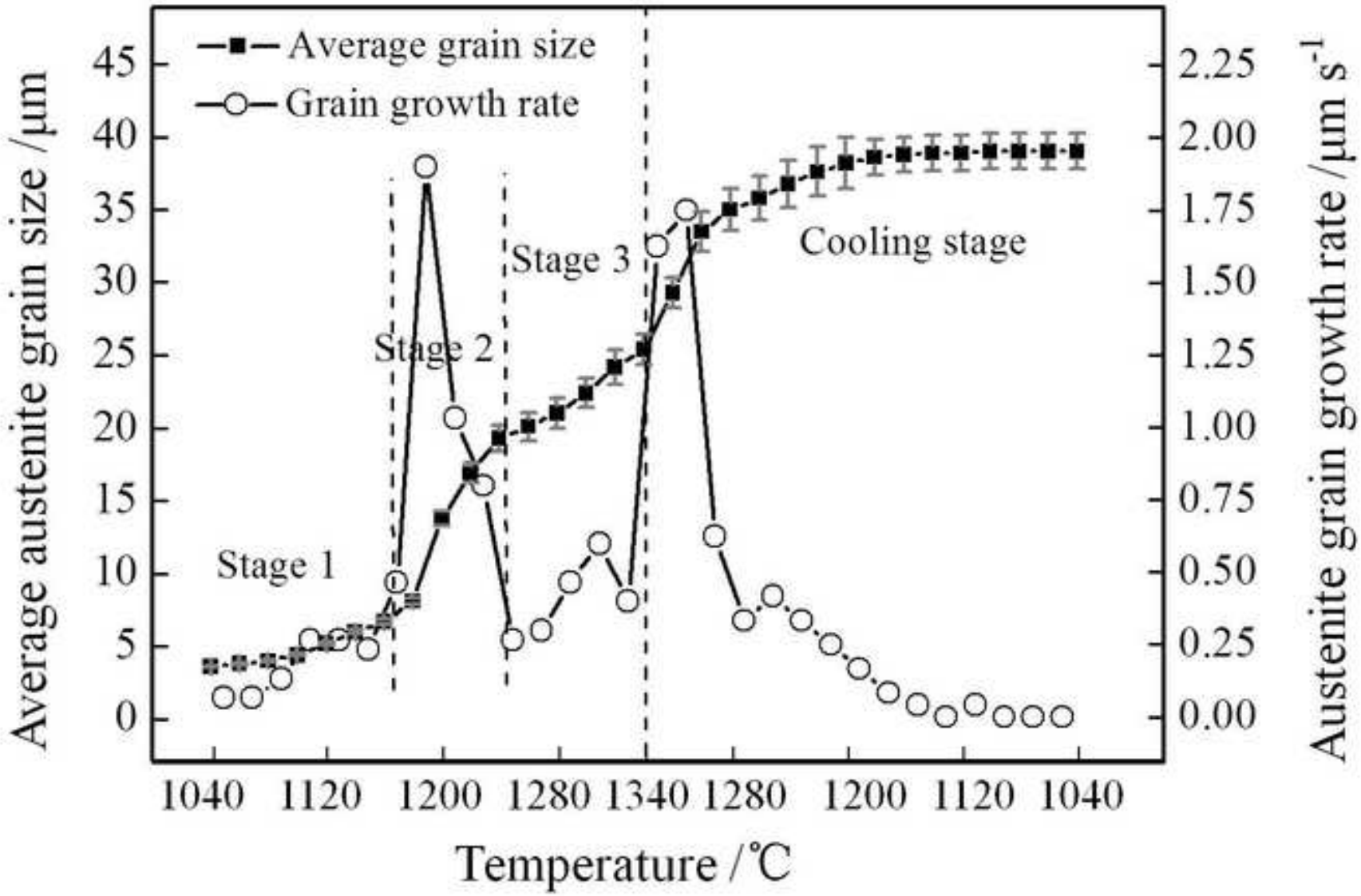

Colour figure
Click here to download high resolution image